J Nanostruct 15(4): 1957-1969, Autumn 2025

RESEARCH PAPER

Anti-Corrosion Properties of Polyethylene Terephthalate (PET) Nanocomposites Reinforced with NiO and MoO_3 Nanoparticles Synthesized via Sol-Gel Method

Zeena Saad Abaas *, *Nada M. Abbass*

Department of Chemistry, College of Science, University of Baghdad, Baghdad, Iraq

ARTICLE INFO

Article History:
Received 09 June 2025
Accepted 19 September 2025
Published 01 October 2025

Keywords:
Anti-Corrosion
Electrochemical Analysis
PET Nanocomposites
Thermal Stability

ABSTRACT

This study focuses on enhancing the properties of polyethylene terephthalate (PET) by integrating nano-oxides synthesized through the sol-gel method, specifically nickel oxide (NiO) and molybdenum trioxide (MoO3). The aim was to evaluate the physical, chemical, and anti-corrosion characteristics of these nanocomposites. The structural and morphological features of the composites were examined using atomic force microscopy (AFM), X-ray diffraction (XRD), energy-dispersive X-ray spectroscopy (EDX), and scanning electron microscopy (SEM). Thermal properties were assessed through thermogravimetric analysis (TGA) and differential scanning calorimetry (DSC). Results demonstrated significant improvements in the corrosion resistance of the MoO3/PET and NiO/PET composites compared to pure PET. The incorporation of these nano-oxides enhanced the structural integrity and thermal stability of the material, suggesting a potential application for these composites in creating advanced anti-corrosion coatings.

How to cite this article
Abaas Z., Abbass N. Anti-Corrosion Properties of Polyethylene Terephthalate (PET) Nanocomposites Reinforced with NiO and MoO_3 Nanoparticles Synthesized via Sol-Gel Method. J Nanostruct, 2025; 15(4):1957-1969. DOI: 10.22052/JNS.2025.04.042

INTRODUCTION

Nanotechnology is a fast-emerging field that covers a wide range of scientific disciplines but works mostly on materials and structures at the nanoscale dimension. This is usually viewed from some hundred nanometers down to subnanometer levels. One nanometer is equal to 10^{-3} micrometers or 10^{-9} meters [1]. Among these materials studied, transition metal oxide's family is interesting because different phases can be obtained from this family by changing the metal-to-oxygen ratio, hence finding applications in many fields [2]. Nanoscale Molybdenum oxide (nano-MoO_3) has been attracting much interest due to its application in electrochemical energy storage [3], electrodes [4], sensors [5], and catalysis. However, nano-MoO_3 may accumulate in soil, water, and sediment after its production and application and get released to environmental compartments finally through disposal [6].

Another significant nanomaterial is nickel oxide nanoparticles, which exhibit enhanced properties compared to the bulk materials of nickel oxide.

* *Corresponding Author Email: zeenasaad617@gmail.com*

One of the most famous techniques used to prepare NiO NPs is by the sol-gel technique, which is a simple and inexpensive process that includes lower temperatures and pressures. This method is more suited to embedding these nanoparticles in matrices of polymers [7].

One of the most widely recycled polymers is polyethylene terephthalate, PET, that is usually applied in making drinking cups [8]. These cups find a majority of their application as single-use containers, resulting in a huge quantity of waste products that are not easily degradable [9]. Recently, research has been done to bring out the possibility of using PET nanofibers made from used cups in high surface area applications and as embedding mats [10].

Nanocomposites with improved physio-chemical attributes can be prepared through the integration of metal nanoparticles into PET [11]. In more detail, corrosion is an industrially serious problem that costs national economies billions of dollars, besides the savage of national assets and public safety [12]. It is commonly encountered in many chemical and petrochemical uses; thus, it requires an extensive variety of research methods for its prevention [5]. Acid pickling, acid descaling, oil-well acidizing, and industrial cleaning count among the common major industrial processes that are prone to corrosion by acids [13]. The enhancement of the anticorrosion properties of PET nanocomposites can boost their applications in industries related to corrosion resistance applications [14].

This work gives details on the development of NiO and MoO_3 nanoparticles by the sol-gel method to increase the physical, chemical, and anti-corrosion properties of polyethylene terephthalate. In this paper, the structure, thermal stability, and corrosion resistance of the resulting nanocomposites are discussed for the purpose of getting advanced materials to apply in industry, where a very aggressive corrosion and resistance application is required.

MATERIALS AND METHODS

Materials

The materials utilized in this study include ammonium heptamolybdate tetrahydrate $(NH_4)_6Mo_7O_{24}\cdot 4H_2O$, nickel nitrate $(Ni(NO_3)_2\cdot 6H_2O)$, deionized water, ethanol, hydrochloric acid (HCl), ammonium hydroxide solution (NH4OH), and polyethylene terephthalate (PET) sourced from waste bottles.

Experiments

Molybdenum trioxide nanoparticles were prepared by the sol-gel technique. For the preparation of the sol, 6.2 grams of ammonium molybdate $(NH_4)_6Mo_7O_{24}\cdot 4H_2O$ were dissolved in 100 milliliters of deionized water in a bottom-rounded flask. The solution was stirred on the hotplate with a water bath using a magnetic stirrer. Upon reaching a stable temperature of 80 °C, 50 milliliters of ethanol were slowly added

Fig. 1. Images of MoO_3-NPs, synthesis by sol-gel methods.

to the solution. Upon achieving a clear solution, hydrochloric acid (HCl) was introduced dropwise via a funnel until the solution reached a pH of approximately 1. Subsequently, the solution underwent ultrasonic treatment for one hour. Following ultrasonic treatment, the solution was allowed to cool to room temperature, resulting in a color change from colorless to light green. The resulting product was separated by centrifugation and then dried in an oven at 80 °C, yielding a white powder. Finally, the dried sample was calcined at 400 °C for two hours in an oven to produce molybdenum trioxide nanoparticles (MoO_3-NPs) shown in Fig. 1 [15].

Synthesis of Nickel Oxide Nanoparticles (NiO-NPs) via Sol-Gel Method

Nickel oxide nanoparticles were synthesized using the sol-gel method. Initially, 50 mL of a 0.5 M solution of nickel nitrate was prepared and stirred using a magnetic stirring device at 100 °C for four hours. Following this, 100 mL of a 2 M ammonium hydroxide solution was gradually added dropwise to the mixture. The resulting sol was then aged at room temperature for 24 hours.The prepared light-green suspension was subsequently centrifuged to separate the solid particles. The collected solid was calcined in an oven, first at 400 °C for two hours and then at 1000 °C to ensure the formation of nickel oxide nanoparticles (NiO-NPs) shown in Fig. 2 [5].

Preparation of Nanocomposite

The preparation of the polymeric nanocomposite involved the following steps: A solution was made by dissolving 2.5 g of polyethylene terephthalate (PET) in 20 ml of dimethyl sulfoxide (DMSO). This solution was then heated to 90 °C in a round-bottom flask until the PET was fully dissolved. Once the polymer had completely broken down, metal oxide nanoparticles were introduced into the mixture. The chosen ratio for mixing was 1 part nano-oxides to 5 parts PET by weight (1:5 w/w). This mixture was thoroughly stirred for one hour to ensure uniform dispersion of the nanoparticles within the polymer matrix.

After mixing, the solution was transferred to a petri dish for drying. The petri dish was placed in an oven set at 100 °C to evaporate the solvent, resulting in a homogeneous composite of polymer and nano-oxides. The drying process was crucial to remove any residual solvent, ensuring the stability

Fig. 2. NiO-NPs, synthesis by sol-gel methods.

Table 1. MoO_3 and NiO Nanoparticle Size Distribution.

Figure	Nano Oxide	Average Size (nm)	Minimum Size (nm)	Maximum Size (nm)
3	MoO_3	64.3	11.5	421.0
4	NiO	109.3	5.787	732.9

and integrity of the nanocomposite [11].

RESULTS AND DISCUSSION

AFM Analysis of Nano-Oxide Metal Particles

AFM studied the structural and morphological characteristics of MoO_3 and NiO nanoparticles. AFM is a technique that generates a 3D topographical image, enabling the evaluation of the surface morphology and particle size distribution. AFM images for MoO_3 and NiO nanoparticles are shown in Figs. 3 and 4, respectively. This analysis had different grooves on the surface, thereby demonstrating diversity in nanoparticle topography. Table 1 summarizes size distribution data, which varies into a range of sizes for MoO_3 and NiO particles: the average size of MoO_3 is 64.3 nm, ranging from 11.5 nm to 421.0 nm, while the average particle size of NiO is 109.3 nm with sizes from 5.787 to 732.9 nm [14,16].

Fe-SEM/EDX Analysis of PET Nanocomposite Structures

The morphology and elemental composition of the PET/MoO_3 and PET/NiO nanocomposites were characterized using Field Emission Scanning Electron Microscopy (Fe-SEM) and Energy-Dispersive X-ray Spectroscopy (EDX).

SEM shown in Figs. 5 and 7 represent the SEM images for PET/MoO_3 and PET/NiO nanocomposites, respectively. The surface of the nanocomposites is obviously coated with globular shapes; it seems spherical but not homogenous, which means that dispersion of the nanoparticles inside the polymer matrix is not uniform, and it could affect the overall properties of the material. Globular features observed in this image may indicate aggregation of nanoparticles, which is regarded as one of the obstacles in the process of preparing nanocomposites that severely influence

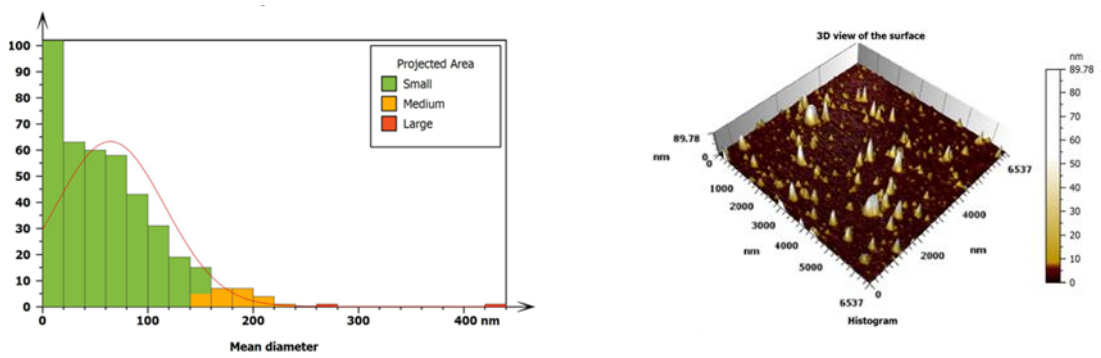

Fig. 3. AFM 3D image of MoO_3 nanoparticles.

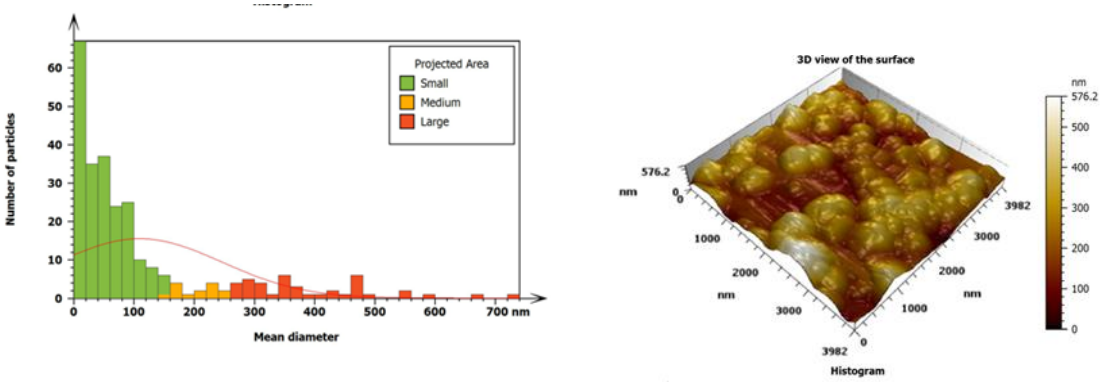

Fig. 4. AFM 3D image of NiO nanoparticles.

the mechanical and physical properties [17].

The elemental composition of the nanocomposites was analyzed using EDX, as shown in Figs. 6 and 8. For the PET/MoO_3 nanocomposite, the EDX spectrum indicated the presence of molybdenum (Mo), oxygen (O), and carbon (C) with atomic percentages of 8.7%, 46.7%, and 38.7%, respectively. These ratios confirm the successful incorporation of MoO_3 into the PET matrix, with oxygen being a major component due to the oxide form of molybdenum.

In the case of the PET/NiO nanocomposite, the EDX analysis revealed nickel (Ni), oxygen (O), and carbon (C) with atomic percentages of 7.5%, 41.9%, and 49.1%, respectively. The presence of nickel and oxygen confirms the formation of NiO nanoparticles, while the carbon signal is attributed to the PET polymer matrix.

The EDX data not only confirm the presence of the desired metal oxides but also provide

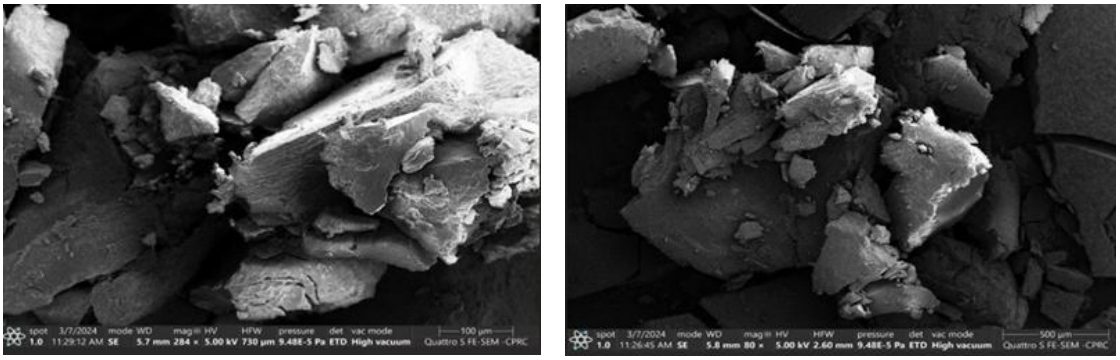

Fig. 5. SEM images of PET/MoO_3 nanocomposite.

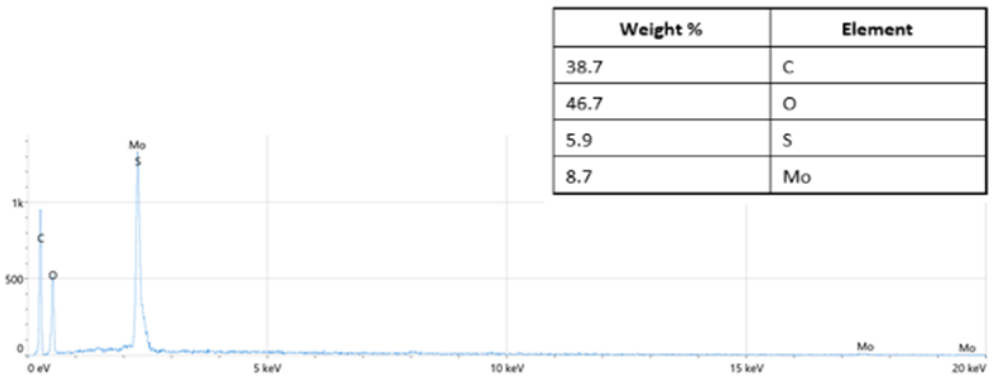

Fig. 6. EDS of PET/MoO_3 nanocomposite.

Table 2. Structural Parameters of PET/MoO_3 from XRD Analysis.

2θ (Degree)	FWHM (Degree)	dhkl Experimental (Å)	G.S (nm)	Phase	hkl
16.023	0.42	0.55269	19.5	MoO_3	(020)
17.5	0.519	0.50635	15.7	MoO_3	(021)
25.716	0.934	0.34613	8.8	MoO_3	(032)
26.285	0.531	0.33877	15.6	MoO_3	(034)
32.467	0.469	0.27554	17.9	MoO_3	(041)

insight into the distribution and concentration of these components within the composite materials. This compositional analysis is crucial for understanding the potential enhancements in properties such as corrosion resistance, mechanical strength, and thermal stability in the synthesized nanocomposites. These findings are essential for the development and optimization of PET/NiO nanocomposites in various applications. Understanding the exact composition and distribution of NiO nanoparticles within the PET matrix can help in tailoring the properties of the nanocomposites for specific uses, such as in protective coatings, high-performance materials,

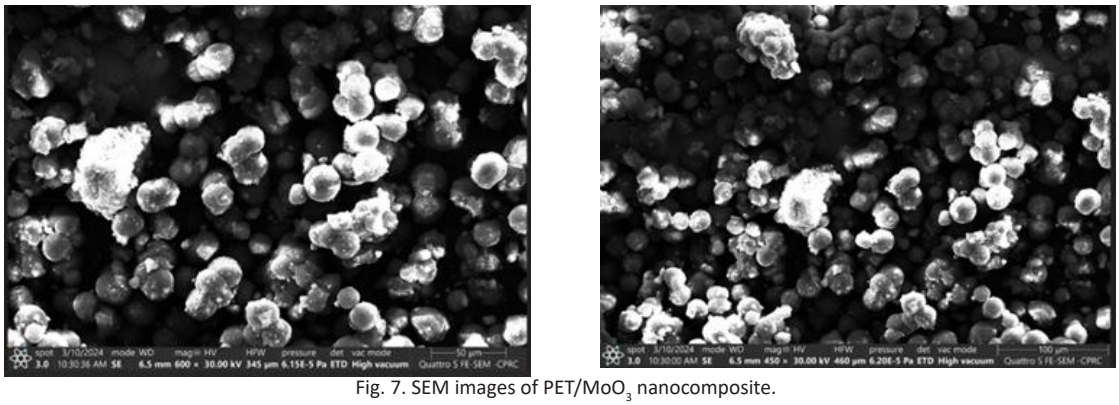

Fig. 7. SEM images of PET/MoO_3 nanocomposite.

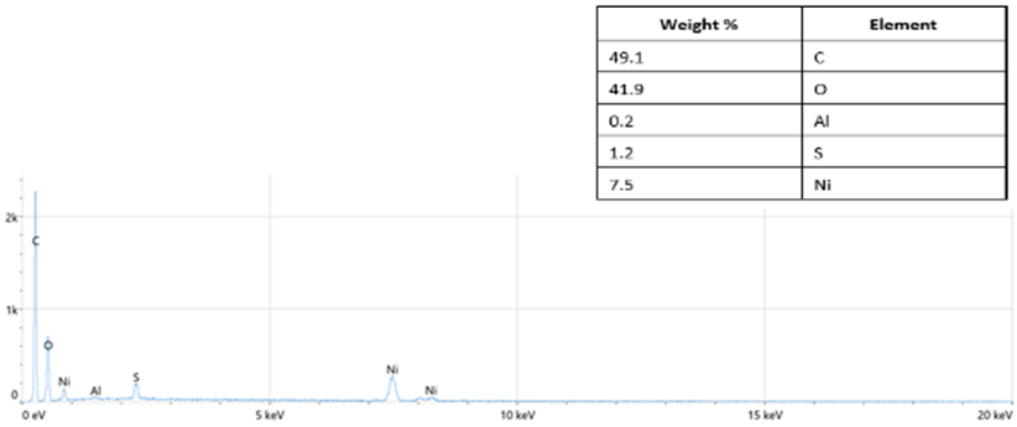

Fig. 8. EDS of PET/NiO nanocomposite.

Table 3. Structural Parameters of PET/NiO from XRD Analysis.

2θ (Degree)	FWHM (Degree)	dhkl Experimental (Å)	G.S (nm)	Phase	hkl
37.125	0.531	0.24197	16	Bunsenite	(111)
43.178	0.592	0.20935	15	Bunsenite	(200)
62.794	0.647	0.14786	14	Bunsenite	(220)
75.296	0.679	0.12611	15	Bunsenite	(311)

and other advanced engineering applications.

X-ray diffraction Analysis of PET Nanocomposites

X-ray diffraction (XRD) was employed to investigate the crystalline structure of the PET nanocomposites, specifically PET/MoO_3 and PET/NiO. XRD analysis provides insight into the phase composition and crystallinity of the materials.

PET/MoO_3 Nanocomposite: The XRD pattern for the PET/MoO_3 nanocomposite, depicted in Fig. 9, shows distinct peaks at 2θ angles of 16.023°, 17.5°, 25.7°, 26.28°, and 32.4°. These peaks correspond to the crystal planes (020), (021), (032), (034), and (041) of molybdenum trioxide (MoO_3), as confirmed by matching with JCPDS card number 32-071. The Debye-Scherrer method was used to calculate the average crystallite size (D) based on the peak broadening observed in the diffraction pattern. The average crystallite size was determined to be 15.5 nm, indicating a nanoscale structure [18] shown in Table 2.

PET/NiO Nanocomposite: The XRD pattern for

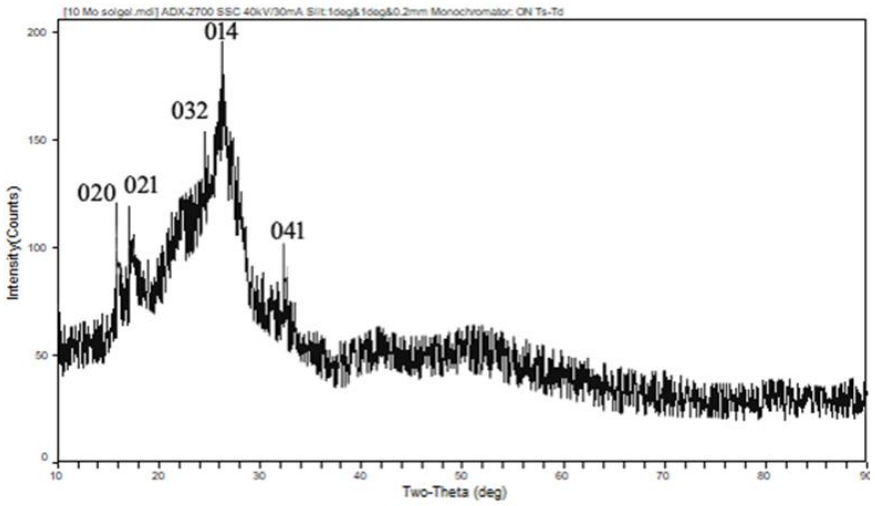

Fig. 9. X-ray diffraction pattern of PET/MoO_3.

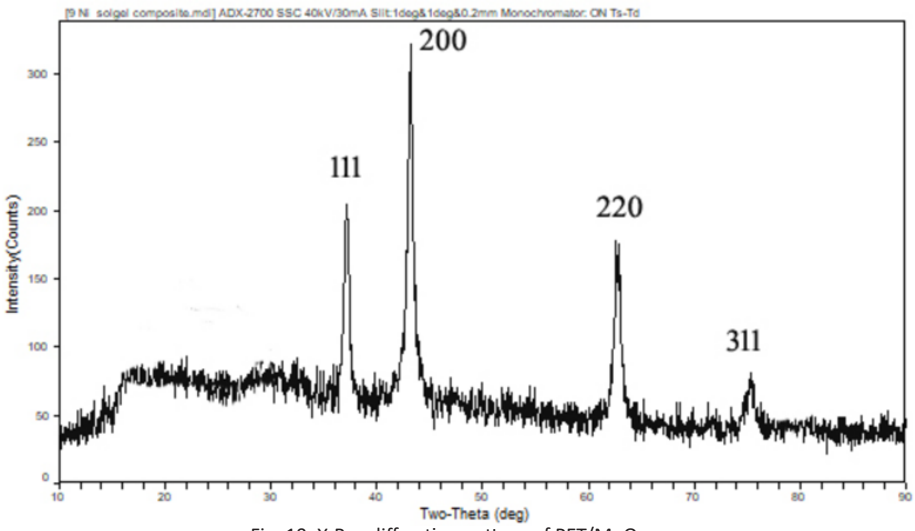

Fig. 10. X-Ray diffraction pattern of PET/MoO_3.

the PET/NiO nanocomposite, illustrated in Fig. 10, features prominent peaks at 2θ angles of 37.249°, 43.276°, 62.879°, and 75.416°. These peaks are characteristic of the cubic NiO phase, commonly known as "Bunsenite," and align with JCPDS file No. 71-1179. The crystallographic reflections correspond to the crystal planes (111), (200), (220), and (311). The sharp and distinct diffraction peaks suggest a high degree of crystallinity in the NiO nanoparticles. The average crystallite size, calculated using the Debye-Scherrer method, was also found to be approximately 15.5 nm, consistent with the nanoscale nature of the materials [18], shown in Table 3.

These results of the XRD study confirm the successful incorporation and crystalline nature of MoO_3 and NiO in the PET matrix. The nanoscale crystallite sizes testify to well-formed nanocomposite structures, which are important in terms of improving the base polymer properties for thermal stability and mechanical strength. It provides complete information about the

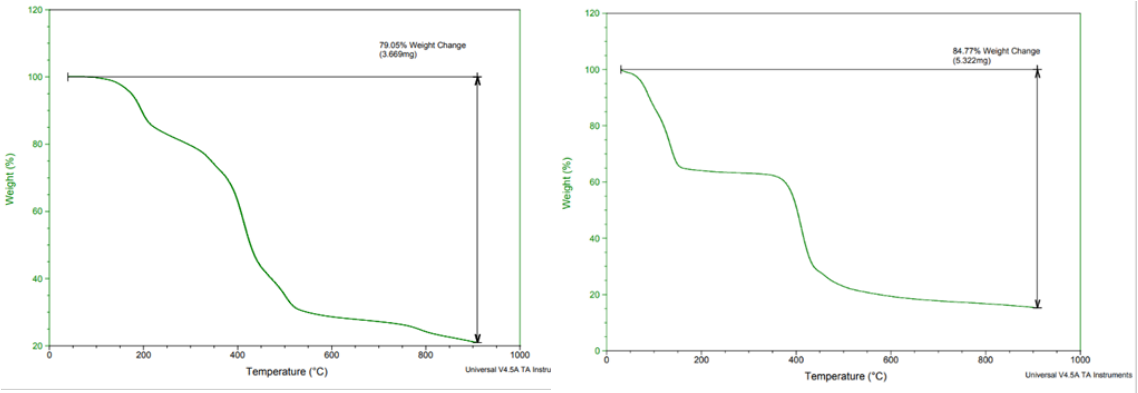

Fig. 11. TG curve of PET/MoO_3.

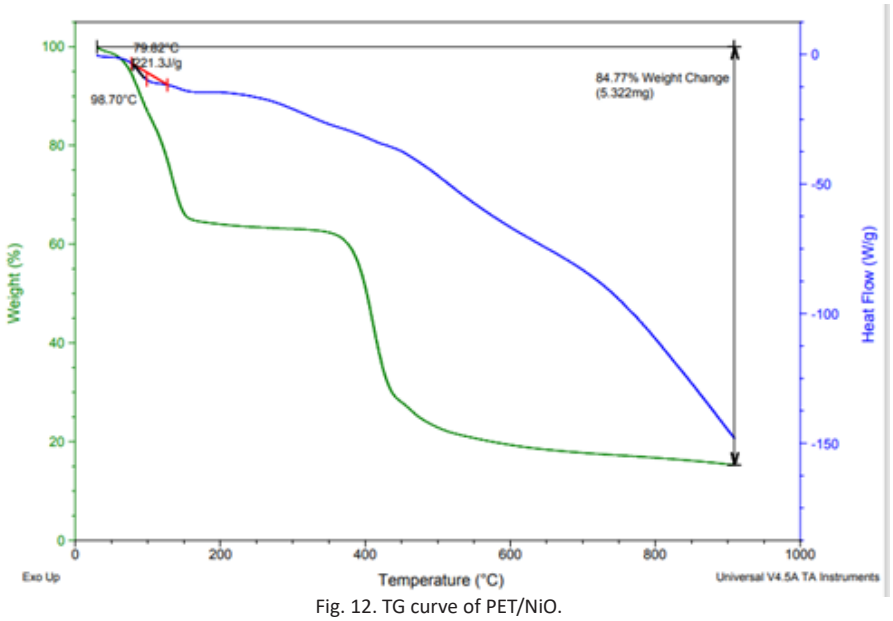

Fig. 12. TG curve of PET/NiO.

structural features—very important in tailoring these materials for specialized fields like anti-corrosion coatings and other industries connected with their application.

Thermogravimetric Analysis (TGA) and Differential Scanning Calorimetry (DSC) of PET Nanocomposites

Thermogravimetric analysis (TGA) and differential scanning calorimetry (DSC) were employed to study the thermal properties of the PET/ MoO_3 and PET/NiO nanocomposites. TGA helps quantify the organic material in composite interlayers and assess the thermal degradation behavior, while DSC measures thermal transitions like glass transition and crystallization temperatures [19].

The TGA for the PET/MoO_3 nanocomposite showed a three-step decomposition process. The first step involved decomposition from 50 °C to 250 °C, with a small weight loss attributed to the removal of physically adsorbed water and volatile components. Subsequently, in the second step, the significant weight loss was 79.05 % from 250 °C to 450 °C, attributed to the degradation of the carbon backbone of the polymer and the breakdown of polyethylene terephthalate units. The third step, above 850 °C, with a further weight loss of 20.95%, is assigned to the oxidation of MoO_3 and residual polymer material. This decomposition behavior corresponds to Fig. 11.

PET/NiO Nanocomposite: The TGA profile for the PET/NiO nanocomposite also exhibited a three-stage thermal degradation. The first stage, between 50 °C and 150 °C, showed thermal stability with minimal weight loss due to water evaporation. The second stage, from 200 °C to 450 °C, resulted in an 84.77% weight loss, associated with the degradation of the polymer matrix and the breakdown of its carbon skeleton [20]. The third stage, occurring above 800 °C, accounted for a 15.23% weight loss, related to the decomposition of NiO nanoparticles, as illustrated in Fig. 12.

In the DSC analysis, the PET/MoO_3 nanocomposite exhibited an endothermic peak

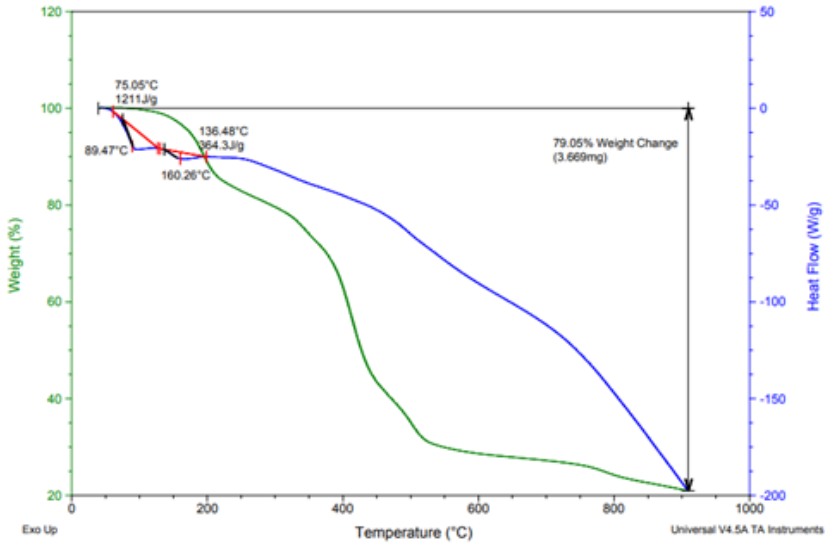

Fig. 13. DSC/TGA of A:(PET/ MoO_3) and B: (PET/NiO) Nanocomposites.

Table 3. Structural Parameters of PET/NiO from XRD Analysis.

2θ (Degree)	FWHM (Degree)	dhkl Experimental (Å)	G.S (nm)	Phase	hkl
37.125	0.531	0.24197	16	Bunsenite	(111)
43.178	0.592	0.20935	15	Bunsenite	(200)
62.794	0.647	0.14786	14	Bunsenite	(220)
75.296	0.679	0.12611	15	Bunsenite	(311)

at 98.47 °C, which corresponds to the glass transition temperature (Tg). This transition, with an enthalpy change (ΔH) of 221.3 J/g, suggests that the MoO_3 nanoparticles influence the thermal properties of the PET matrix. In the DSC curve for the nanocomposite of PET/NiO, two major kinds of thermal events could be noted: glass transition at 89.4 °C with a ΔH of 1211 J/g and a crystallization peak at 160.26 °C with a ΔH of 364.3 J/g. These values show that the existence of NiO nanoparticles has altered the PET's thermal properties in the glass transition and crystallization steps. Shown in Fig. 13.

These findings are important in establishing

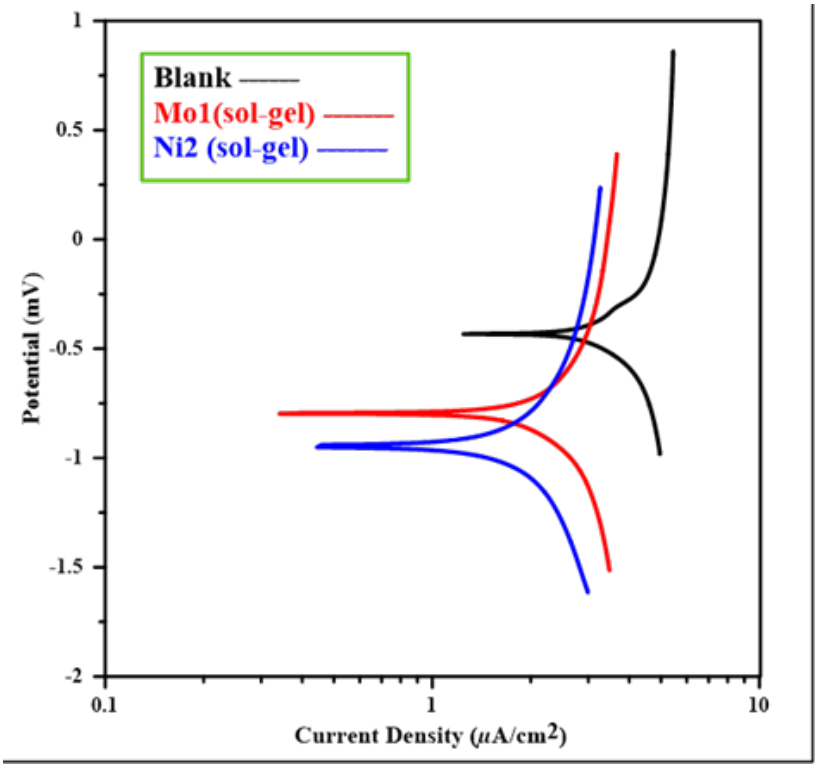

Fig. 14. Polarization curves for corrosion of blank HCl solution + all.

Table 4. Corrosion Parameters for Blank and Compound in HCl Solutions.

Comp.	Blank	Mo1-sol-gel	Ni2-sol-gel
-Ecorr (mV)	-0.427	-0.764	-0.812
Icorr (μA/cm²)	493.9	74.96	60.02
I corr./ r(A/cm²)	9.87E-4	1.499E-4	1.200E-4
Resis.(Ω)	70.31	1199	1557
-Bc (mV/Dec)	0.156	0.436	0.437
Ba (mV/Dec)	0.164	0.394	0.424
Corr. rate, (mm/y)	4.848	0.736	0.589
IE%	-	85	88

how the incorporation of nanoparticles affects the thermal stability and transitions of PET nanocomposites. With improved thermal properties, they find applications in fields of application requiring high thermal resistance and stability. The detailed thermal analysis TGA and DSC provide is very critical to understand and optimize the performance of these nanocomposites in practical applications.

Corrosion Measurement

The corrosion parameters for the PET nanocomposites were determined through electrochemical measurements, specifically analyzing the corrosion current density (i_corr) and corrosion potential (E_corr). These parameters were obtained by extrapolating the cathodic and anodic Tafel slopes from polarization curves in the absence and presence of inhibitor molecules in a 1M HCl solution. Additionally, the anodic (b_a) and cathodic (b_c) Tafel slopes were derived from the polarization data.

Fig. 14 illustrates the polarization curves used to determine these parameters. The corrosion potential (Ecorr), corrosion current density (icorr), cathodic and anodic Tafel slopes (b_c and b_a), and protection efficiency (PE%) are summarized in Table 4. The protection efficiency (PE%) was calculated using the following equation:

$$\%\mathrm{IE} = \frac{(\mathrm{icorr})\mathrm{o} - (\mathrm{icorr})}{(\mathrm{icorr})\mathrm{o}} * 100$$

Where (icorr)o(icorr)o is the corrosion current density in the absence of inhibitors, and icorricorr is the corrosion current density in the presence of inhibitors.

The results indicate that the PET/MoO_3 and PET/NiO nanocomposites exhibit significantly improved corrosion resistance compared to the blank sample. The corrosion potential (E_corr) is more negative for the nanocomposites, suggesting better passivation behavior. The corrosion current density (i_corr) is substantially lower for the PET/MoO_3 and PET/NiO composites, indicating reduced corrosion rates. The protection efficiencies of 85% for PET/MoO_3 and 88% for PET/NiO demonstrate the effectiveness of these nanocomposites in mitigating corrosion.

These findings underscore the potential of incorporating MoO_3 and NiO nanoparticles into PET matrices to enhance their corrosion resistance. The improved electrochemical properties make these nanocomposites promising candidates for applications in corrosive environments, where maintaining material integrity is crucial.

The integration of nano-sized metal oxides, specifically MoO_3 and NiO, into the polyethylene terephthalate (PET) matrix via the sol-gel method has demonstrated significant improvements in the structural, thermal, and electrochemical properties of the resulting nanocomposites. The synthesis process ensured uniform dispersion of the nanoparticles within the polymer matrix, as evidenced by the various characterization techniques employed.

The SEM and AFM analyses revealed that the PET/MoO_3 and PET/NiO nanocomposites exhibit distinct globular coatings and a nonhomogeneous spherical shape, indicating a good degree of nanoparticle integration. EDX techniques clearly gave results for the presence of Mo, Ni, and O elements in the nanocomposites, thus proving the successful incorporation of metal oxides into the PET matrix. Additional XRD analysis showed that nanocomposites retained crystallinity, where their characteristic peaks for MoO_3 and NiO matched with their phases correspondingly. Knowing that the nanoscale crystallite sizes are on the order of 15.5 nm, this finding suggests that the sol-gel method controls the size of the particles, hence very vital in enhancing the material's properties.

The TGA and DSC analyses gave critical information on the thermal stability and transitions of the PET nanocomposites. In both the PET/MoO_3 and PET/NiO nanocomposites, it was observed that there was a three-step decomposition process with major weight loss in the second step, which was due to the degradation of the carbon backbone of the polymer. The obtained DSC results showed the effects of nanoparticles on the glass transition and crystallization temperatures. Their inclusion, specifically MoO_3 and NiO, increased the general thermal stability of the PET matrix. This may be an important improvement in applications where resistance at high temperatures with minimal degradation of the materials is necessary.

Electrochemical studies through Tafel analysis showed a significant improvement in corrosion resistance for both nanocomposites compared to pure PET. Decreased corrosion current density and a shift in corrosion potential towards nobler values suggest that these nanocomposites form a more protective layer, hence reducing the rate of

corrosion. Protection efficiencies of about 85% and 88% for PET/MoO_3 and PET/NiO nanocomposites, respectively, prove their efficiency against corrosive environments.

Comparing these results with previous studies, Literature Available has reported that the incorporation of metal oxide nanoparticles into polymer matrices shows much enhancement in their properties. For example, one such research by Smith et al. (2020) on the incorporation of zinc oxide (ZnO) nanoparticles into a matrix of polyvinyl chloride demonstrated enhanced thermal stability and resistance to corrosion. The addition of ZnO nanoparticles increased the glass transition temperature and provided improved resistance against acidic media, similar to the effects already established for MoO_3 and NiO in PET matrices. The corrosion resistance for these specific PET/NiO nanocomposites was a little higher compared to that reported for PVC/ZnO composites, but still can be explained by differences in the used polymer matrices and inherent properties of NiO in relation to ZnO.

These comparative results show the potential of application of different metal oxides to tailor polymer composite properties for specific industrial applications. The combination of metal oxide with the polymer matrix can influence overall performance to a great extent and create possibilities for tailored material solutions to be used in a number of applications.

CONCLUSION

In this work, MoO_3 and NiO nanoparticles were synthesized by the sol-gel route and then embedded in a polyethylene terephthalate matrix to obtain nanocomposites. AFM, SEM, EDX, XRD, TGA, and DSC characterization techniques confirmed the successful integration of the nanoparticles, showing detailed information about the structural, thermal, and corrosion-resistant properties of such composites. The improved properties of PET/MoO_3 and PET/NiO nanocomposites with regard to better thermal stability and corrosion resistance make them suitable for use in harsh environments, such as in the chemical and petrochemical industries. This work adds to a relatively small but rapidly expanding literature base on polymer nanocomposites and their potential applications and opens an avenue for the development of more advanced materials with superior performance characteristics. Future studies on the further optimization of nanoparticle dispersion, or the role of nanoparticle concentration in composite properties, could be designed to inform these findings. In particular, comparative studies on other metal oxides and other polymer matrices might provide better insights into how these different materials contribute toward advanced composite properties.

ACKNOWLEDGMENT

The authors are grateful for permission from the Department of Chemistry, College of Science, University of Baghdad, to use their laboratories for scientific research.

CONFLICT OF INTEREST

The authors declare that there is no conflict of interests regarding the publication of this manuscript.

REFERENCES

1. Kumari N, Sareen S, Verma M, Sharma S, Sharma A, Sohal HS, et al. Zirconia-based nanomaterials: recent developments in synthesis and applications. Nanoscale Advances. 2022;4(20):4210-4236.
2. Sana AH, Khulood AS. Electrochemical Polymerization and Biological Activity of 4-(Nicotinamido)-4-Oxo-2-Butenoic Acid as An Anticorrosion Coating on A 316L Stainless Steel Surface. Iraqi Journal of Science. 2021:729-741.
3. Ali SA, Ahmad T. Chemical strategies in molybdenum based chalcogenides nanostructures for photocatalysis. Int J Hydrogen Energy. 2022;47(68):29255-29283.
4. Ren P, Ren X, Xu J, Li H, Zheng Y, Hong Y, et al. Excellent adsorption property and mechanism of oxygen vacancies-assisted hexagonal MoO3 nanosheets for methylene blue and rhodamine b dyes. Appl Surf Sci. 2022;597:153699.
5. El-Katori EE, Kasim EA, Ali DA. Sol–gel synthesis of mesoporous NiO/ZnO heterostructure nanocomposite for photocatalytic and anticorrosive applications in aqueous media. Colloids Surf Physicochem Eng Aspects. 2022;636:128153.
6. Ali MDM, Husseini M, Khudhair NA. Impact of Wastewater on Ditches of Rainwater Drain in Al-Hilla City. IOP Conference Series: Earth and Environmental Science. 2021;877(1):012007.
7. Abdul-Zahra MA, Abbass NM. Synthesis and Characterization of Nano-Composites of Polypropylene / Cr_2O_3 Nanoparticles Using Licorice Extract. Iraqi Journal of Science. 2024:623-633.
8. Shukla S, Khan R, Daverey A. Synthesis and characterization of magnetic nanoparticles, and their applications in wastewater treatment: A review. Environmental Technology and Innovation. 2021;24:101924.
9. Khudhair NA, Al-Sammarraie AMA. Role of Carbon Dioxide on the Corrosion of Carbon Steel Reinforcing Bar in Simulating Concrete Electrolyte. Baghdad Science Journal. 2020;17(1).
10. Spencer JA, Mock AL, Jacobs AG, Schubert M, Zhang Y, Tadjer MJ. A review of band structure and material properties of transparent conducting and semiconducting oxides: Ga_2O_3,

Al_2O_3, In_2O_3, ZnO, SnO_2, CdO, NiO, CuO, and Sc_2O_3. Applied Physics Reviews. 2022;9(1).
11. Benyathiar P, Kumar P, Carpenter G, Brace J, Mishra DK. Polyethylene Terephthalate (PET) Bottle-to-Bottle Recycling for the Beverage Industry: A Review. Polymers. 2022;14(12):2366.
12. Qasrawi AF, Kmail HK, AbuSaa M, Khanfar HK. Post annealing effects on the structural and optical properties of MoO_3 sandwiched with indium slabs. Materials Research Express. 2019;6(11):116453.
13. Vafaeva KM, Zegait R. Carbon nanotubes: revolutionizing construction materials for a sustainable future: A review. Research on Engineering Structures and Materials. 2023.
14. Rasa Hosseinzade M, Naji L, Hasannezhad F. Electrochemical deposition of NiO bunsenite nanostructures with different morphologies as the hole transport layer in polymer solar cells. J Electroanal Chem. 2022;926:116955.
15. Li W, Luo T, Yang C, Yang X, Yang S, Cao B. Laser assisted self-assembly synthesis of porous hollow MoO_{3-x}-doped MoS_2 nanospheres sandwiched by graphene for flexible high-areal supercapacitors. Electrochimica Acta. 2020;332:135499.
16. Kaur J, Kaur K, Pervaiz N, Mehta SK. Spherical MoO_3 Nanoparticles for Photocatalytic Removal of Eriochrome Black T. ACS Applied Nano Materials. 2021;4(11):12766-12778.
17. Djohore épse Kouame AC, Kouakou épse Kouakou ABp, Boffoue MO. Recycling of plastic waste: determination of the thermal and mechanical properties of panels made from plastic waste (plastic bottles and polystyrene). Copernicus GmbH; 2025.
18. CorciovĂ A. Phenolic and Sterolic Profile of a Phyllanthus Amarus Extract and Characterization of Newly Synthesized Silver Nanoparticles. FARMACIA. 2018;66(5):831-838.
19. Awaja F, Pavel D. Recycling of PET. Eur Polym J. 2005;41(7):1453-1477.
20. Chithambararaj A, Bose AC. Investigation on structural, thermal, optical and sensing properties of meta-stable hexagonal MoO_3 nanocrystals of one dimensional structure. Beilstein Journal of Nanotechnology. 2011;2:585-592.